RESEARCH   **Open Access**

Astrocyte tau deposition in progressive supranuclear palsy is associated with dysregulation of *MAPT* transcription

Rosemary J. Jackson[1], Alexandra Melloni[1], Dustin P. Fykstra[1], Alberto Serrano-Pozo[1], Leslie Shinobu[2] and Bradley T. Hyman[1]*

Abstract

Progressive supranuclear palsy (PSP) is a neurodegenerative disease characterized by 4R tau deposition in neurons as well as in astrocytes and oligodendrocytes. While astrocytic tau deposits are rarely observed in normal aging (so-called aging-related tau astrogliopathy, ARTAG) and Alzheimer's disease (AD), astrocytic tau in the form of tufted astrocytes is a pathognomonic hallmark of PSP. Classical biochemical experiments emphasized tau synthesis in neurons in the central nervous system, suggesting that astrocytic tau inclusions might be derived from uptake of extracellular neuronal-derived tau. However, recent single-nucleus RNAseq experiments highlight the fact that *MAPT*, the gene encoding tau, is also expressed by astrocytes, albeit in lower amounts. We, therefore, revisited the question of whether astrocyte-driven expression of tau might contribute to astrocytic tau aggregates in PSP by performing fluorescent in situ hybridization/immunohistochemical co-localization in human postmortem brain specimens from individuals with PSP and AD with ARTAG as well as normal controls. We find that, in PSP but not in AD, tau-immunoreactive astrocytes have higher levels of *MAPT* mRNA compared to astrocytes that do not have tau aggregates. These results suggest that astrocytic responses in PSP are unique to this tauopathy and support the possibility that fundamental changes in PSP astrocyte-endogenous mRNA biology contribute to increased synthesis of tau protein and underlies the formation of the astrocytic tau deposits characteristic of PSP.

Keywords Progressive supranuclear palsy, Astrocytes, MAPT, Tufted astrocytes, Tau

Introduction

Progressive supranuclear palsy (PSP) is one of a number of neurogenerative tauopathies distinguished from each other by unique neuropathological features and hallmarks [15, 16]. Although all the primary tauopathies are characterized by hyperphosphorylation and aggregation of the cytoskeletal protein tau, these diseases differ from each other in the regional distribution, cell type, morphology, and structure of these aggregates. Arguably, fundamental differences in underlying tau biology underscore these disease-specific characteristics and translate into the distinct clinical phenotypes associated with each of these diseases.

Tau protein is encoded by the *MAPT* gene, which contains a number of splice sites leading to tau isoforms of different lengths. Inclusion of exon 10 encodes four repeat (4R) tau which contains a fourth microtubule binding domain and generates a protein critically

*Correspondence:
Bradley T. Hyman
bhyman@mgh.harvard.edu
[1]Massachusetts General Hospital, 114 16th Street, Charlestown, MA 02129, USA
[2]Bristol Myers Squibb, Neuroscience Thematic Research Center, 250 Water Street, Charlestown, MA 02141, USA

different from the three repeat (3R) tau variant lacking that extra microtubule binding repeat motif [2, 11].

Biochemically, the tau aggregates in PSP mainly contain 4R tau [2, 11, 12, 26] while anatomically, tau aggregates in astrocytes are pathognomonic of PSP although tau inclusions are also found in neurons, predominantly in the brainstem and motor-related subcortical structures [15, 16]. By contrast, in Alzheimer's disease (AD) tau deposits contain a mixture of 3R and 4R tau, occur primarily in limbic and cortical structures, and are predominantly neuronal, although occasional astrocytic tau inclusions can be observed—collectively termed age-related tau astrogliopathy (ARTAG) [12, 16]. The morphology of tau-containing astrocytes is also distinctive, with tufted astrocytes defining PSP and thorn-shaped astrocytes being the main morphology in ARTAG [13]. Since astrocytic tau inclusions have been observed to correlate with synaptic alterations in PSP and corticobasal degeneration (CBD) and synaptic changes are amongst the earliest drivers of altered/failing function in neurodegenerative disease, the importance of understanding the origin and functional impact of astrocytic inclusions is of high interest.

Why tau accumulates in distinct cell types in the various tauopathies remains unknown. Tau is considered a member of the metastable subproteome—a set of highly expressed and aggregation-prone proteins whose normal function relies on a delicate equilibrium between gene expression levels and homeostasis of the cellular proteostasis systems [3, 17]. Therefore, one possibility is that an increased *MAPT* gene expression within astrocytes is a major driver of tau accumulation in PSP tufted astrocytes. Indeed, the idea that tau expression might be related to the development of neuropathology in PSP is supported by several lines of evidence. Polymorphisms in the *MAPT* gene are linked to enhanced neuropathological changes, especially oligodendroglial coiled bodies and tufted astrocytes [12]. In particular, the H1 haplotype of *MAPT* is associated with a predisposition to develop PSP [4, 10]. Previous work in mouse models has shown that overexpression of human *MAPT* in astrocytes is sufficient to induce tau pathology reminiscent of PSP in these cells [5, 7]. Recent human PSP single-nucleus RNA-sequencing (snRNA-seq) datasets show that the *MAPT* gene is expressed in the central nervous system primarily in neurons, but that glia—especially astrocytes—do show readily detectable levels of *MAPT* mRNA [28]. We reasoned that astrocytes that develop inclusions in PSP either have a unique ability to take up and accumulate tau from the extracellular environment or, plausibly, begin to overexpress the *MAPT* gene in response to as yet unidentified triggers, leading to enhanced synthesis of the tau protein beyond their clearance capacity, resulting in the development of the pathognomonic tau inclusions.

To begin to test which of these potential mechanisms underlies astrocytic tau accumulation in PSP we developed methods to perform fluorescent in situ hybridization and concurrent immunohistochemistry to allow spatial resolution of *MAPT* mRNA transcripts in human postmortem brain tissue. We compared individuals with PSP and AD with ARTAG, and asked if astrocyte (or neuronal) *MAPT* mRNA levels are increased in the subset of neurons or astrocytes that develop tau inclusions relative to those that do not. We observed an increase in *MAPT* mRNA specifically in astrocytes containing tau inclusions in PSP, but not in AD with ARTAG, suggesting the possibility that a dysregulation of tau gene expression contributes to the accumulation of tau in the tufted astrocytes characteristic of PSP.

Materials and methods
Brain donors
Frozen samples and 7 μm-thick formalin-fixed paraffin-embedded (FFPE) sections from the striatum and frontal association cortex of age- and sex-balanced 10 PSP, 9 AD, and 5 normal controls were obtained from the Massachusetts Alzheimer's Disease Research Center (MADRC) Neuropathology Core brain bank. PSP donors met current neuropathological diagnostic criteria for PSP [23]. AD donors met current clinical and neuropathological diagnostic criteria for AD [18] but were selected to have astrocytic tau inclusions consistent with ARTAG [14, 20]. Normal control donors did not have any clinical symptoms of any neurodegenerative disease during life and did not meet neuropathological diagnostic criteria for any neurodegenerative disease at autopsy examination. All donors or their next-of-kin provided informed written consent for the brain donation, which was conducted under the MADRC Neuropathology Core Institutional Review Board protocol. Approximatively, 0.5 g of frozen frontal cortex or striatum were dissected and kept at −80 °C until processing. Case information is in Table 1.

Immunohistochemistry with peroxidase-DAB
We performed automated immunohistochemistry (IHC) for phospho-Tau (Ser202, Thr205) antibody (clone AT8, ThermoFisher Scientific #MN1020, 1:2,000) in FFPE sections from the striatum and frontal cortex with the peroxidase-3,3′-diaminobenzidine (DAB) method using a Leica BOND Polymer Refine Detection kit (Leica Biosystems, DS9800) in a Leica BOND RX Fully Automated Research Stainer (Leica Biosystems). Immunostained sections were then scanned in a VS-120 Olympus slide scanner under the 40x objective.

Table 1 Human brain donor information

ADRC #	Age at Death	Sex	NPDX1	NPDX2	NPDX3	H1/H2 Genotype	ApoE Genotype	TDP-43 Pathology	Braak Stage	Thal Stage	Processed			
											Astro Striatum	Astro FC	Neuro Striatum	Neuro FC
1967	70	Male	AD	CAA	CVD	H1/H1	4/4	No	V	5	x	x	x	x
2144	65	Male	AD	CVD		H1/H2	3/3	No	VI	5			x	x
2229	75	Female	AD			H1/H2	3/4	Yes	VI	5	x	x	x	x
2262	74	Male	AD	TDP	CAA	genotyping declined	genotyping declined	Yes	VI	5	x	x	x	x
2333	79	Male	AD	CAA	CVD	H1/H1	3/4		V	5	x	x		x
2354	72	Female	AD	TDP	HS	H1/H2	3/3	Yes	VI	5	x	x		
2382	58	Female	AD	CVD		H1/H1	3/3	No	VI	5	x	x		x
2391	74	Female	AD	CVD	LBD	H1/H1	4/4	Yes	VI	5	x	x	x	x
2400	73	Female	AD	CAA	CVD	H1/H1	3/4	No	V	5	x	x	x	x
1893	81	Female	Control	INF	CVD	H1/H2	3/3		I	3	x	x		
2407	59	Male	Control		CVD	H1/H2	2/4	No	0	0	x	x	x	x
2463	63	Male	Control	CVD	Acute Hypoxia	genotyping declined	genotyping declined		0	2	x	x	x	x
2465	73	Male	Control	CVD	Acute Hypoxia	genotyping decline	genotyping decline		0	2	x	x	x	x
2477	68	Female	Control	CVD		genotyping declined	genotyping declined	No	I	0	x	x	x	x
1668	69	Male	PSP	CVD		H1/H1	3/4		N/A	N/A	x	x	x	x
1991	78	Male	PSP	Hemorrhage		H1/H1	2/3	No	II		x	x	x	x
2047	63	Female	PSP			H1/H1	3/4						x	
2163	89	Female	PSP	CVD		H1/H1	3/4	No	0	0	x	x		
2183	69	Male	PSP	HS		H1/H1	3/3	Yes	0		x	x	x	x
2196	>=90	Male	PSP			H1/H2	3/3	No	0	0	x	x	x	
2296	78	Female	PSP	CVD		H1/H1	3/3	No				x	x	x
2320	71	Female	PSP	CVD		H1/H1	2/3	No	N/A	N/A		x	x	x
2423	77	Female	PSP	CVD		H1/H1	2/3	No	0	0	x	x	x	x
2529	72	Male	PSP	CVD	Acute Hypoxia	H1/H1	2/3	Yes	N/A	N/A	x	x	x	x

AD: Alzheimer's Disease, PSP: Progressive Supranuclear Palsy, CAA: Cerebral Amyloid Angiopathy, CVD: Cerebrovascular Disease, INF: Infarcts,

TDP: TDP-43 Proteinopathy Unspecified, HS: Hippocampal Sclerosis, LBD: Lewy Body Disease

Fluorescence in situ hybridization assay

RNAScope

We performed the RNAScope protocol using the RNAscope multiplex fluorescent assay v2 kit (ACD #323100) and following the manufacturer instructions for frozen tissue. Briefly, brains were cut on a cryostat to a thickness of 8 μm and then mounted onto Superfrost slides (Fisher Scientific) with three sections per slide. Sections were immersed in 4% paraformaldehyde at 4 °C for 15 min and then dehydrated through increasing ethanol gradient. Slides were then allowed to dry at room temperature (RT) and sections were outlined with a hydrophobic pen. Samples were then exposed to RNAScope Hydrogen Peroxide solution (ACD #322335) for 10 min at RT followed by a 5-minute incubation in RNAScope protease IV (ACD #322340).

Sections were then incubated with probes for 2 h at 40 °C. The following probes were used in different combinations and were run alongside a negative control probe (ACD #320871) and a positive control probe Hs-*UBC* (ACD #310041). *SLC1A2* was used as a marker of astrocytes while *SYP* was used as a marker for neurons.

Combination 1: Hs-*MAPT* (ACD #408991) and Hs-*SLC1A2*-C3 (ACD #444721-C3).

Combination 2: Hs-*MAPT* (ACD #408991) and Hs-*SYP*-C3 (ACD #311421-C3).

Combination 3: Hs-*MAPT* (ACD #408991), Hs-*MAPT-AS1*-C2 (ACD # 564491-C2), and Hs-*SLC1A2*-C3 (ACD #444721-C3).

Combination 4: Hs-*MAPT* (ACD #408991), Hs-*MAPT-AS1*-C2 (ACD # 564491-C2), and Hs-*SYP*-C3 (ACD #311421-C3).

Following probe incubation, consecutive amplification steps were performed in the same oven using the RNAScope Multiplex FL v2 kit. C1 probes were developed using TSA Plus Cy3 (Akoya Biosciences, #NEL744E001KT), C3 probes with TSA Plus Fluorescein (Akoya Biosciences, #NEL741001KT), and C2 probes (when applicable) with TSA Plus Cy5 (Akoya Biosciences, #NEL745E001KT).

Autofluorescence quenching

Immediately following the final step of RNAScope kit the sections were washed 3 times in tris-buffered saline (TBS). To quench tissue autofluorescence, sections were then incubated in 1x TrueBlack (Biotium 23007) in 70% ethanol for 30 s at RT before immediately being washed 3 times in TBS. Sections were never allowed to dry out and were processed in small batches to minimize tissue autofluorescence.

RNA quality control

For all slides, a positive control probe for *UBC* (encoding ubiquitin C) was run on an adjacent section and used to determine RNA integrity with strict cut-offs. Because RNA integrity varied between brain regions and was lost over time following sectioning, slides which failed this quality control test were not processed for further analysis (Table 1 shows details of which donors were used for each analysis).

Fluorescent immunohistochemistry

The samples were then processed for an IHC assay using the monoclonal mouse phospho-Tau (Ser202, Thr205) antibody (clone AT8, ThermoFisher Scientific #MN1020). Briefly samples were blocked in 5% Normal Donkey Serum (NDS) for 1 h at RT followed by overnight incubation with AT8 antibody (1:500) in 2.5% NDS in TBS. Sections were washed and then incubated with donkey anti-mouse IgG Alexa Fluor 750 (Abcam AB175738) 1:200) in 2.5% NDS in TBS for 1 h at RT. Sections were then washed and counterstained with 1:1,000 DAPI in TBS for 5 min and mounted using Immu-Mount (Fisher Scientific, 9990402). Immunostained sections were scanned in a VS-120 Olympus slide scanner with the 40x objective for all relevant channels.

QuPath image analyses

Images were loaded directly into QuPath open access image analysis software [1] and areas of grey matter were outlined manually. Positive cell detection was used on all annotated areas detecting nuclei using the DAPI channel allowing split by shape. Cell expansion was set at 5 μm and the cell outlines included the cell nucleus. Astrocytes and neurons were identified in the FITC channel by their *SLC1A2* and *SYP* expression, respectively, since C3 probes were visualized with TSA Plus Fluorescein. A single threshold of mean FITC staining in the nucleus was used per image to delineate astrocytes or neurons as appropriate. Although this number differed on a donor-by-donor basis depending on background and staining integrity, the experimenter assigning this threshold was blind to diagnosis and only FITC and DAPI channels were used in the determination of an appropriate cut-off.

Subcellular detection was used to quantify the number of transcripts for *MAPT* and *MAPT-AS1* [24]. The expected mean spot size was $1\mu m^2$ (range 0.5-2.0μm^2). When two spots or more spots were clustered together they were split first by intensity and then by size to achieve the appropriate number of transcripts. Again, exact detection thresholds varied depending on background and signal intensity but were decided by a blinded experimenter using only the relevant channel. A case-wise cut-off value for AT8 signal intensity were variably applied but was again determined by a blinded investigator.
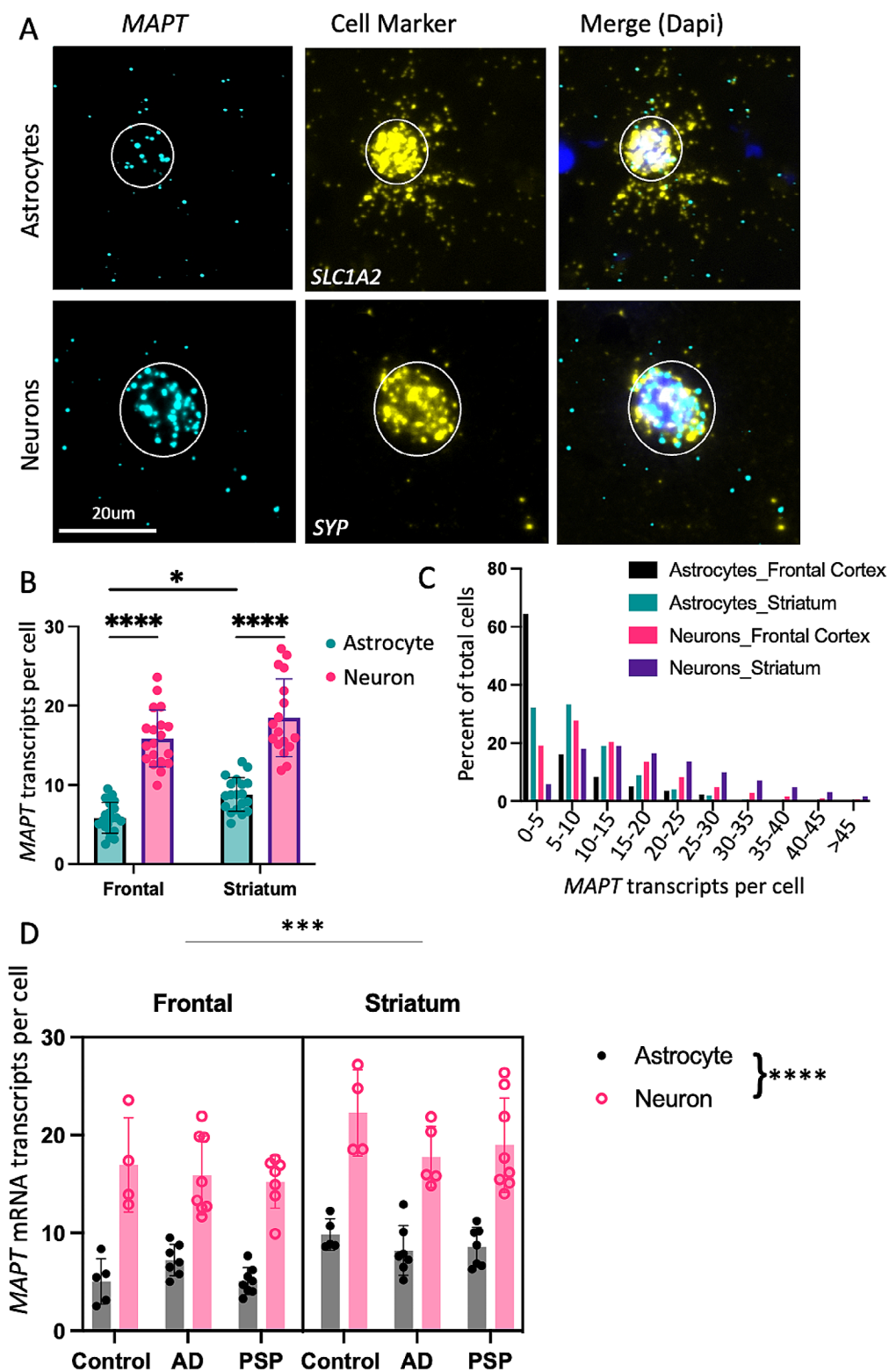
Fig. 1 *MAPT* transcripts are found in both neurons and astrocytes regardless of diagnosis. (**A**) RNAScope probes for *MAPT* (cyan), *SLC1A2* (yellow, marker of astrocytes), and *SYP* (yellow, marker for neurons) transcripts as well as DAPI (blue). (**B**) Quantification of average *MAPT* transcript number for each donor per cell type in frontal cortex vs. striatum. (**C**) Histogram showing the distribution of *MAPT* transcript number for all cells per brain area. Number displayed represents the bin center, bins are 5 wide. (**D**) Average number of *MAPT* transcripts per donor shows a significant difference between neurons vs. astrocytes and striatum vs. frontal cortex, but no difference across the three diagnoses. (*$p < 0.05$,***$p < 0.001$,****$p < 0.0001$)
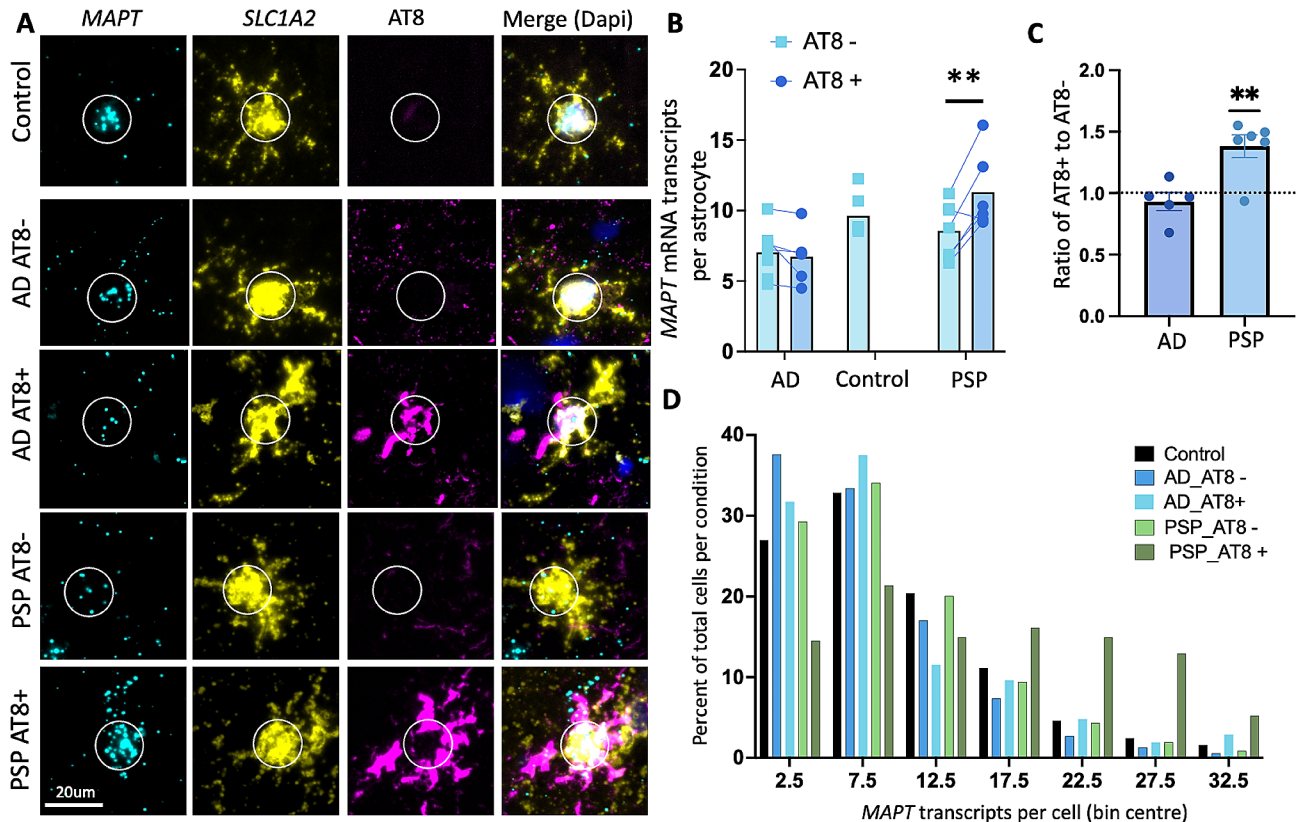
Fig. 2 *MAPT* transcript number is increased in AT8-positive astrocytes in the striatum. (**A**) RNAScope for *MAPT* (cyan) and *SLC1A2* (yellow, marker of astrocytes) transcripts as well as IHC for AT8 (magenta, marker of hyperphosphorylated tau) and DAPI (blue). (**B**) Average number of *MAPT* transcripts per cell for AT8+ and AT8- show a significant increase *MAPT* expression in PSP but not in the other diagnoses (dot shows average per donor). (**C**) Ratio of average *MAPT* expression of AT8+ to AT8- cells per donor shows a significant increase in PSP but not AD (one-way ANOVA to 1, graph shows mean +/- SEM). (**D**) Histogram showing the distribution of *MAPT* transcript number for all cells per condition and AT8 designation. Number displayed represents the bin centre, bin width is 5. (**p < 0.01)

Statistical analyses

GraphPad Prism v10.0.2 (Dotmatics, Boston, MA) was used for all statistical analyses and graphs. Mean transcript number per case was determined for astrocyte and neurons in the different brain regions for all cells that were either AT8- or AT8+. For donors with less than ten AT8+ cells this value was excluded although the AT8- value was still used for statistics. Individual donors are summarized by a single average data point and graphs show mean +/- SD unless otherwise indicated. Histograms were generated using cells from all cases for each designation as indicated on the graph and are binned as indicated. Repeated measures mixed effect model was used to determine an effect of AT8 positivity on *MAPT* and *MAPT-AS1* transcript number with disease state as the row effect and AT8 status as the column effect. Uncorrected Fisher's LSD was used as a post-hoc test for these analyses. The same test was used to assess *SLC1A2* intensity in astrocytes. Ratios were analyzed using a one-tail t-test or one-way ANOVA against a theoretical mean of 1 (a ratio of 1 indicating no difference between AT8- and AT8+).

Results

We utilized RNAscope, an in situ hybridization technique which allows for highly specific single transcript detection with excellent spatial resolution, in postmortem brain tissue collected from control, AD with ARTAG, and PSP individuals (Table 1 and Supplemental Fig. S1) [27]. Probes used were designed for *MAPT* (all tau isoforms) as well as *SLC1A2* (encoding the astrocyte-specific glutamate transporter EAAT2/GLT-1) and *SYP* (encoding the neuron-specific synaptophysin) (Fig. 1A) [29]. We found a robust number of *MAPT* transcripts in both the nucleus and cytoplasm of astrocytes in all three conditions. Using the positive cell detection method on QuPath, cells were identified based on DAPI staining, then expanded by 5 μm, and then marked as astrocytes or neurons depending on the intensity of the RNA marker for each of those cell types (i.e., *SLC1A2* vs. *SYP* respectively), [1]. We then quantified the number of *MAPT* transcripts in those cells using the subcellular detection method. Quantification showed a significantly higher number of *MAPT* transcripts in neurons vs. astrocytes ($p < 0.0001$, F (3, 71) = 68.64); the number of
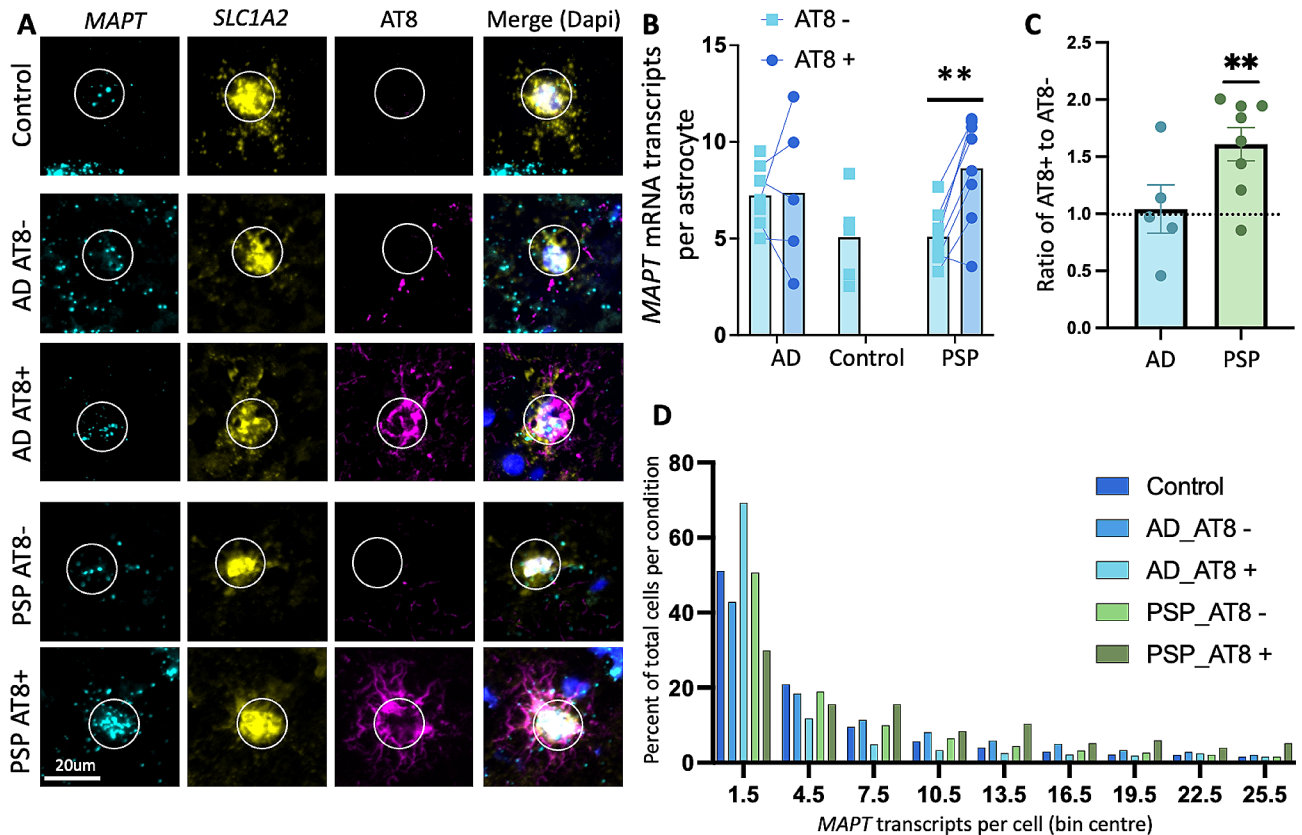
Fig. 3 *MAPT* transcript number differs in AT8 positive vs. negative astrocytes in the frontal cortex. **(A)** RNAscope for *MAPT* (cyan) and *SLC1A2* (yellow, marker of astrocytes) transcripts as well as IHC for AT8 (magenta, marker of hyperphosphorylated tau) and DAPI. **(B)** Average number of *MAPT* transcripts per AT8 + and AT8- cell show a significantly increased *MAPT* expression in PSP but not other conditions (dots show average per donor) **(C)** Ratio of average *MAPT* expression of AT8 + to AT8- cells per donor shows a significant increase in PSP but not AD (one-way ANOVA to 1, graph shows mean +/- SEM) **(D)** Histogram showing the distribution of *MAPT* transcript number for all cells per condition and AT8 designation. Number displayed represents the bin center, bin width is 3. (**$p < 0.01$)

MAPT transcripts per astrocyte was ~ 30–50% relative to that of neurons and higher in astrocytes from striatum than frontal cortex (FC) ($p = 0.0280$) (Fig. 1B). The transcript number did not seem to be affected by diagnosis ($p = 0.2380$) (Fig. 1D). Interestingly, there were twice as many astrocytes with >5 transcripts of *MAPT* in striatum vs. FC (~70% vs. ~35%), revealing regional differences that may contribute to selective vulnerability to tau aggregation (Fig. 1C).

In PSP, astrocyte tau pathology can precede neuronal tau pathology in some brain regions, including specifically in the striatum [16]. Therefore, we asked if striatal astrocytes in which *MAPT* expression is higher than average might be the same astrocytes bearing tau pathology before any such neuronal pathology is seen. To investigate this, we combined RNAscope for *MAPT* and *SLC1A2* probes with IHC for the phospho-tau epitope AT8 (Fig. 2A) and classified astrocytes into AT8 + and AT8- depending on their AT8 staining intensity. We found significantly more *MAPT* transcripts in AT8 + vs. AT8- astrocytes in PSP but not in AD with ARTAG

donors (Interaction factor F (2, 9) = 5.129, PSP AT8+ vs. PSP AT8- $p = 0.0012$) (Fig. 2B). AT8 + astrocytes in PSP had on average 50% more *MAPT* transcripts when compared with AT8- astrocytes from the same donor, whereas AT8 + astrocytes did not show this difference in AD with ARTAG donors—although these had substantially fewer AT8 + astrocytes than PSP donors (t = 4.187, df = 5, $p = 0.0086$) (Fig. 2C). This increase in *MAPT* transcripts in AT8 + astrocytes in PSP donors was driven by a dramatic increase in the proportion of cells with a high number of *MAPT* transcripts (Fig. 2D). For example, only 5% of astrocytes in the control donors had more than 23 *MAPT* transcripts while over 20% of AT8 + PSP astrocytes had more than 23 *MAPT* transcripts (Supplemental Fig. S2A).

We also examined astrocytes in the frontal cortex and found a similar phenomenon (Fig. 3A). In PSP donors, AT8 + astrocytes were found to have on average 50% more *MAPT* transcripts compared to AT8- astrocytes from the same donors (Interaction factor F (2, 9) = 7.962, PSP AT8+ vs. PSP AT8- $p = 0.0036$) (Fig. 3B, C). However,
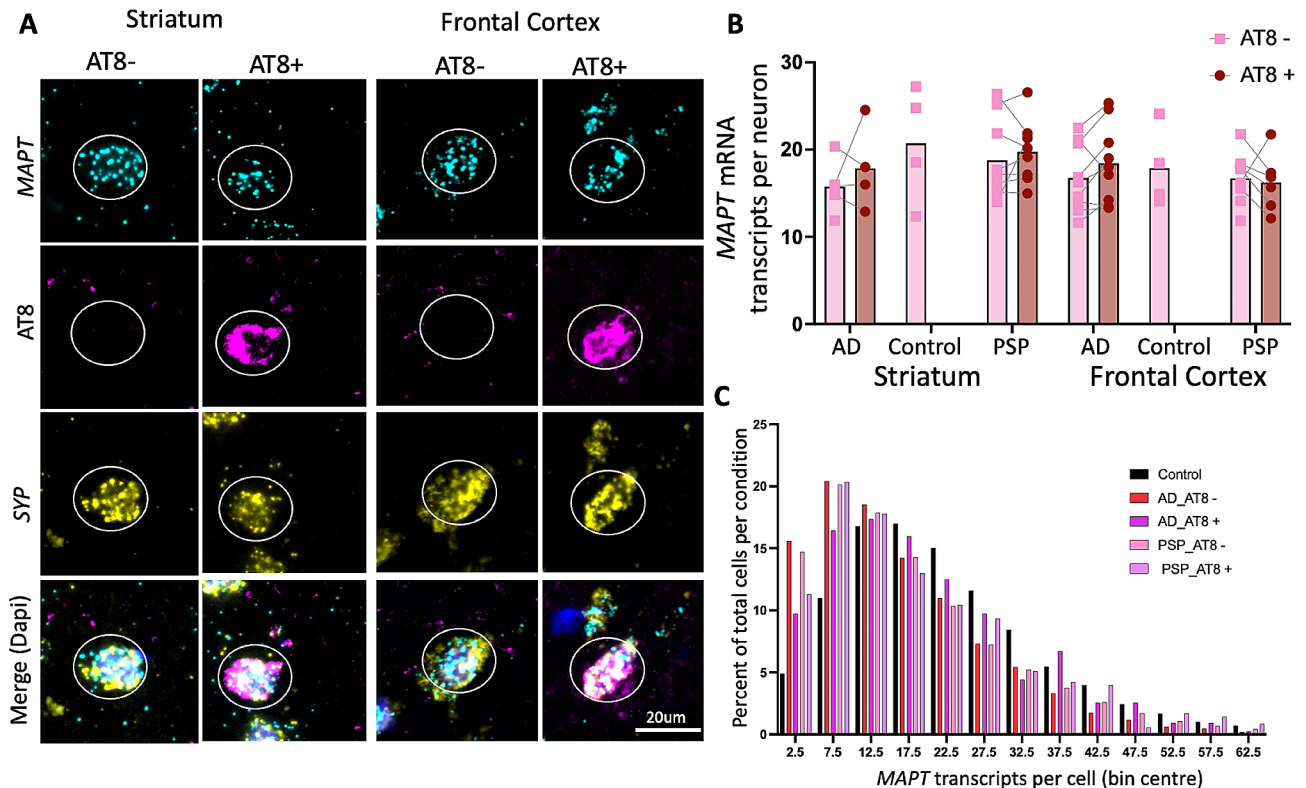
Fig. 4 *MAPT* transcript number in neurons. **(A)** RNAscope for *MAPT* (cyan) and *SYP* (yellow, marker of neurons) transcripts as well as IHC for AT8 (magenta, marker of hyperphosphorylated tau) and DAPI. **(B)** Average number of *MAPT* transcripts for AT8 + and AT8- neurons shows no difference in *MAPT* expression across diagnoses. **(D)** Histogram showing the distribution of *MAPT* transcript number for all cells per condition and AT8 designation in the frontal cortex. Number displayed represents the bin centre, bin width is 5

this difference appeared to be driven by a smaller number of astrocytes with very high *MAPT* transcript levels (Fig. 3D, Supplemental Fig. S2B) and FC astrocytes appeared to make less *MAPT* overall.

Importantly there was no difference in the intensity of *SLC1A2* staining across the groups indicating that this increase in *MAPT* transcript level is due neither to a general increase in all mRNA transcripts in AT8 + astrocytes nor to a technical artifact whereby AT8 + astrocytes were better stained or imaged (Supplemental Fig. S3A). Crucially, when we quantified the intensity of *MAPT* probe staining, PSP astrocytes designated as AT8 + had significantly higher *MAPT* intensity when compared with AT8- intensity from that same donor (Supplemental Fig. S3B), further reinforcing our conclusions.

Previous reports have shown no increase in *MAPT* levels in neurons with tau inclusions in AD [21]. To investigate if this increase in *MAPT* transcripts in PSP astrocytes was specific to astrocytes or also occurred in tangle-bearing neurons, we used RNAscope to probe for *MAPT* and *SYP* (as a marker of neurons) followed by IHC for AT8 (Fig. 4A). In agreement with this previous report, we saw no difference in *MAPT* transcript levels in AT8 + neurons compared to AT8- neurons in AD with ARTAG donors. Here we have extended this finding to

PSP as we observed no increased in *MAPT* transcript level in AT8 + vs. AT8- neurons in either striatum or FC of PSP donors (Fig. 4B, C).

MAPT-AS1 is a recently discovered naturally occurring antisense oligonucleotide that has been postulated to impact the expression of *MAPT* potentially leading to neurodegenerative phenotypes [25]. To assess if *MAPT-AS1* dysregulation could be driving this increase in *MAPT* transcript levels in AT8 + astrocytes from PSP donors we used RNAscope to probe for *MAPT-AS1* and *MAPT* alongside either *SYP* (for neurons) or *SLC1A2* (for astrocytes) followed by IHC with AT8 (Fig. 5A). We found significantly more *MAPT-AS1* transcripts (mixed model, $p=0.0030$) in neurons than in astrocytes, the majority of which had no *MAPT-AS1* at all, however there was no association between *MAPT-AS1* transcript number and AT8 immunoreactivity in any of the three conditions (Fig. 5B-C).

Discussion

Recent snRNA-seq studies suggest that dysregulation of transcriptional activity is correlated with tau deposition [22, 28]. We reasoned that this mechanism could lead to enhanced *MAPT* gene expression in astrocytes and, subsequently, higher chance of tau deposition (i.e., tufted
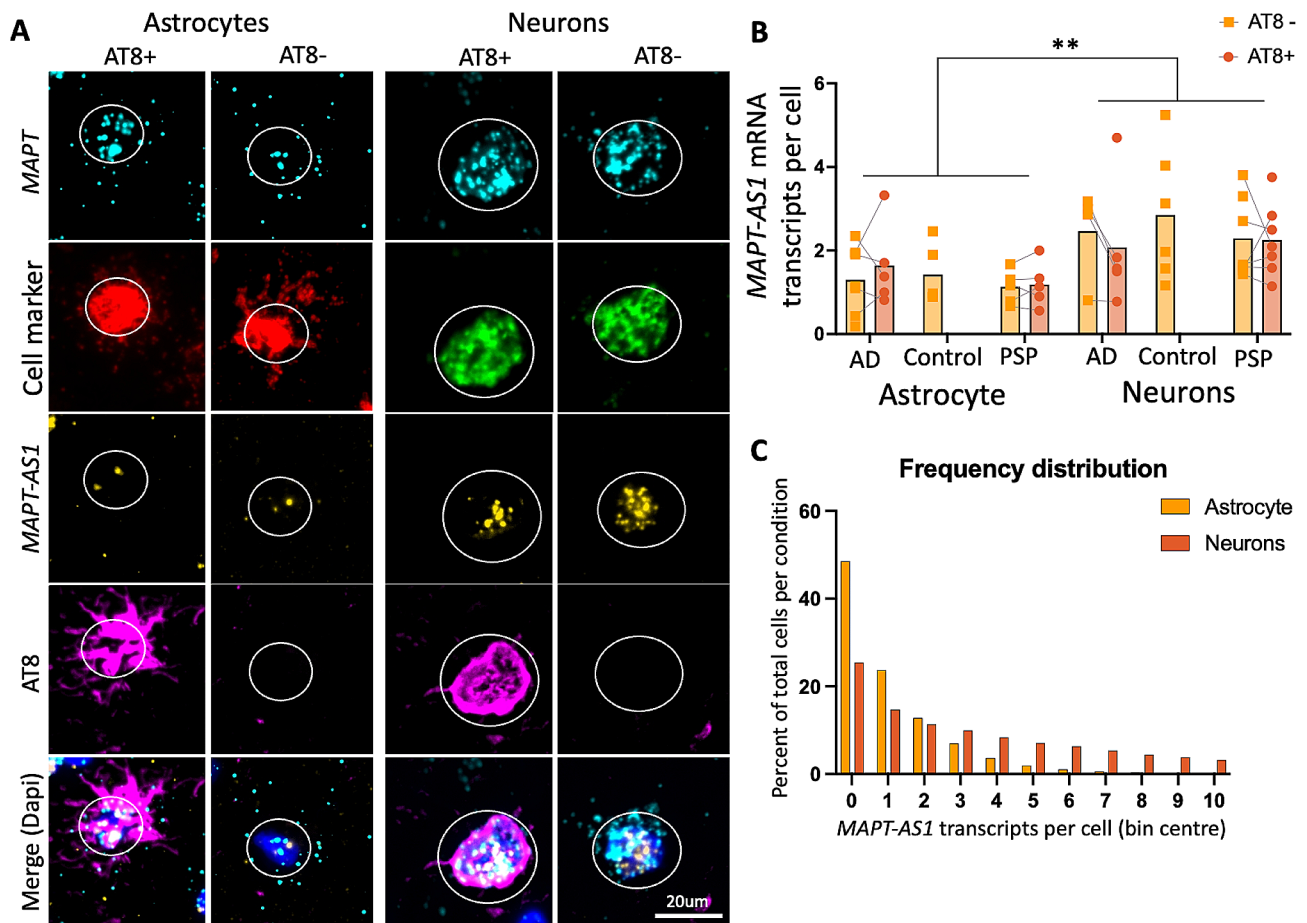
Fig. 5 *MAPT-AS1* transcript number. **(A)** RNAScope for *MAPT* (cyan), *MAPT-AS1* (yellow) and *SYP* (green, marker of neurons) or *SLC1A2* (red, marker of astrocytes) transcripts as well as IHC for AT8 (magenta, marker of hyperphosphorylated tau) and DAPI (blue, merge contains DAPI but not the cell marker for clarity). **(B)** Average number of *MAPT-AS1* transcripts is greater in neurons than astrocytes but does not differ across diagnoses or by the presence of AT8+tau. **(C)** Histogram showing the distribution of *MAPT-AS1* transcript number for all cells per condition and AT8 designation. Number displayed represents the bin centre. *MAPT-AS1* was quantified in the striatum

astrocytes). Thus, we performed in situ hybridization and concurrent IHC to explore the possibility that *MAPT* gene expression would be disrupted in tufted astrocytes in PSP. We found that in PSP brains, astrocytes bearing tau pathology expressed more *MAPT* than astrocytes lacking tau pathology. As a control for both a nonspecific feature of reactive astrocytes and for a closely related but independent tauopathy, we explored *MAPT* expression in selected AD brains which also had tau positive astrocytes (ARTAG) [20]. Interestingly, we found that in AD astrocytes with tau pathology there was no such increase in *MAPT* expression, suggesting different mechanisms of astrocytic tau accumulation in these two tauopathies (i.e., increased transcription and synthesis vs. uptake from extracellular space). Regarding neurons, we saw no change in *MAPT* expression in AT8+ vs. AT8- neurons in either PSP or AD, implying different mechanisms of astrocytic vs. neuronal tau accumulation in PSP.

Substantial upregulation of *MAPT* in a subset of PSP astrocytes correlated with the presence of phosphorylated tau in these cells. This does not appear to reflect technical issues with measuring mRNA in these cells, as we found no significant relationship between *MAPT-AS1* and *MAPT* transcript number in neurons or astrocytes in these cases. Intriguingly, a recent snRNA-seq dataset has shown an impact of H1/H2 haplotype on the expression of *MAPT* in astrocytes [9], and the H1 haplotype is strongly associated with propensity to develop PSP. While it is an interesting possibility that this haplotype may contribute to the altered *MAPT* expression observed in our PSP donors, the current study was not sufficiently powered to examine the effect of the H1/H2 haplotype.

Two recent studies have examined astrocyte *MAPT* expression in PSP. In the first, Fiock et al. using human inducible pluripotent stem cells (hiPSc)-derived astrocytes reported a preferential uptake of 4R compared to 3R recombinant tau [6], suggesting another reason for the

accumulation of 4R tau in astrocytes. This study also performed an analysis similar to ours, using in situ hybridization for *MAPT* combined with GFAP and AT8 IHC to determine tau positive and tau negative astrocytes in PSP brain donors. Four individuals were studied, with an average of over 3,000 astrocytes/donor, and no difference in *MAPT* expression was observed between PSP astrocytes that contained tau protein inclusions and those that did not. The reason for the discrepancy between Fiock et al.'s data and the current study is not clear, but we note that only ~ 50% of astrocytes in their study had detectable *MAPT* mRNA, while snRNA-seq data suggest that essentially all astrocytes express *MAPT* [8], raising the possibility of lower detection sensitivity. In the second recent study, Forrest et al. used RNAScope in situ hybridization combined with AT8 IHC to explore *MAPT* expression in neurons, oligodendroglia, and astrocytes in three control and three PSP donors [8]. In accord with the current results, FC tufted astrocytes contained statistically significantly more *MAPT* mRNA than non-tau containing astrocytes in two of the three PSP donors, and the third donor appeared to have quantitatively more *MAPT* mRNA as well, although the pooled astrocyte results did not reach statistical significance [8]. Moreover, one of the three donors did have statistically significantly higher expression of *MAPT* in tufted astrocytes vs. non-tau containing astrocytes in the basal ganglia. Interestingly, in the same study, *MAPT* expression was significantly higher in coiled body-containing oligodendroglia than in tau-negative oligodendroglia, indicating a similar mechanism in these two glial cell types [8]. Here we have used a much larger cohort of donors with robust quality controls for RNA integrity to expand upon these data and confirm that tufted astrocytes in PSP show an increase in *MAPT* expression while thorn-shaped astrocytes typical of ARTAG in AD do not, indicating different mechanisms of astrocytic tau accumulation in these two diseases.

Taken together, the current data support the idea that a dysregulation of *MAPT* expression occurs in tufted astrocytes that accumulate tau aggregates in PSP. Whether this reflects astrocyte-specific stress responses in PSP, unique genetic risk factors associated with *MAPT* expression that correlate with the risk to develop PSP, or astrocyte-neuron interactions specific to the neurodegenerative environment associated with PSP remains uncertain, but the observations presented here suggest that altered astrocytic *MAPT* expression is a key feature of the molecular biology underpinning disease progression in PSP and should be considered in the context of potential pathologic molecular "drivers" and "ensconces" of disease progression in this tauopathy. Moreover, our findings lend support to the therapeutic approach of lowering *MAPT* expression in PSP with antisense oligonucleotides [19].

References
1. Bankhead P, Loughrey MB, Fernández JA, Dombrowski Y, McArt DG, Dunne PD, McQuaid S, Gray RT, Murray LJ, Coleman HG, James JA, Salto-Tellez M, Hamilton PW (2017) QuPath: open source software for digital pathology image analysis. Sci Rep 7:16878. https://doi.org/10.1038/s41598-017-17204-5
2. Bowles KR, Pugh DA, Oja L-M, Jadow BM, Farrell K, Whitney K, Sharma A, Cherry JD, Raj T, Pereira AC, Crary JF, Goate AM (2022) Dysregulated coordination of MAPT exon 2 and exon 10 splicing underlies different tau pathologies in PSP and AD. Acta Neuropathol 143:225–243. https://doi.org/10.1007/s00401-021-02392-2
3. Ciryam P, Kundra R, Freer R, Morimoto RI, Dobson CM, Vendruscolo M (2016) A transcriptional signature of Alzheimer's disease is associated with a metastable subproteome at risk for aggregation. Proc Natl Acad Sci U S A 113:4753–4758. https://doi.org/10.1073/pnas.1516604113
4. Conrad C, Andreadis A, Trojanowski JQ, Dickson DW, Kang D, Chen X, Wiederholt W, Hansen L, Masliah E, Thal LJ, Katzman R, Xia Y, Saitoh T (1997) Genetic evidence for the involvement of tau in progressive supranuclear palsy. Ann Neurol 41:277–281. https://doi.org/10.1002/ana.410410222

5.   Ezerskiy LA, Schoch KM, Sato C, Beltcheva M, Horie K, Rigo F, Martynowicz R, Karch CM, Bateman RJ, Miller TM (2022) Astrocytic 4R tau expression drives astrocyte reactivity and dysfunction. JCI Insight 7:e152012. https://doi.org/10.1172/jci.insight.152012

6.   Fiock KL, Hook JN, Hefti MM (2023) Determinants of astrocytic pathology in stem cell models of primary tauopathies. Acta Neuropathol Commun 11:161. https://doi.org/10.1186/s40478-023-01655-1

7.   Forman MS, Lal D, Zhang B, Dabir DV, Swanson E, Lee VM-Y, Trojanowski JQ (2005) Transgenic Mouse Model of Tau Pathology in astrocytes leading to Nervous System Degeneration. J Neurosci 25:3539–3550. https://doi.org/10.1523/JNEUROSCI.0081-05.2005

8.   Forrest SL, Lee S, Nassir N, Martinez-Valbuena I, Sackmann V, Li J, Ahmed A, Tartaglia MC, Ittner LM, Lang AE, Uddin M, Kovacs GG (2023) Cell-specific MAPT gene expression is preserved in neuronal and glial tau cytopathologies in progressive supranuclear palsy. Acta Neuropathol 146:395–414. https://doi.org/10.1007/s00401-023-02604-x

9.   Fujita M, Gao Z, Zeng L, McCabe C, White CC, Ng B, Green GS, Rozenblatt-Rosen O, Phillips D, Amir-Zilberstein L, Lee H, Pearse RV, Khan A, Vardarajan BN, Kiryluk K, Ye CJ, Klein H-U, Wang G, Regev A, Habib N, Schneider JA, Wang Y, Young-Pearse T, Mostafavi S, Bennett DA, Menon V, De Jager PL (2024) Cell subtype-specific effects of genetic variation in the Alzheimer's disease brain. Nat Genet 1–10. https://doi.org/10.1038/s41588-024-01685-y

10. Heckman MG, Brennan RR, Labbé C, Soto AI, Koga S, DeTure MA, Murray ME, Petersen RC, Boeve BF, van Gerpen JA, Uitti RJ, Wszolek ZK, Rademakers R, Dickson DW, Ross OA (2019) Association of MAPT Subhaplotypes with Risk of Progressive Supranuclear Palsy and Severity of Tau Pathology. JAMA Neurol 76:710–717. https://doi.org/10.1001/jamaneurol.2019.0250

11. Ikeda C, Yokota O, Miki T, Takenoshita S, Ishizu H, Terada S, Yamada N (2018) Astrocytic tau pathologies in Argyrophilic Grain Disease and Related four-repeat tauopathies. Acta Med Okayama 72:211–221. https://doi.org/10.18926/AMO/56066

12. Ingelsson M, Ramasamy K, Russ C, Freeman SH, Orne J, Raju S, Matsui T, Growdon JH, Frosch MP, Ghetti B, Brown RH, Irizarry MC, Hyman BT (2007) Increase in the relative expression of tau with four microtubule binding repeat regions in frontotemporal lobar degeneration and progressive supranuclear palsy brains. Acta Neuropathol 114:471–479. https://doi.org/10.1007/s00401-007-0280-z

13. Kovacs GG (2020) Astroglia and Tau: New perspectives. Front Aging Neurosci 12:96. https://doi.org/10.3389/fnagi.2020.00096

14. Kovacs GG, Ferrer I, Grinberg LT, Alafuzoff I, Attems J, Budka H, Cairns NJ, Crary JF, Duyckaerts C, Ghetti B, Halliday GM, Ironside JW, Love S, Mackenzie IR, Munoz DG, Murray ME, Nelson PT, Takahashi H, Trojanowski JQ, Ansorge O, Arzberger T, Baborie A, Beach TG, Bieniek KF, Bigio EH, Bodi I, Dugger BN, Feany M, Gelpi E, Gentleman SM, Giaccone G, Hatanpaa KJ, Heale R, Hof PR, Hofer M, Hortobágyi T, Jellinger K, Jicha GA, Ince P, Kofler J, Kövari E, Kril JJ, Mann DM, Matej R, McKee AC, McLean C, Milenkovic I, Montine TJ, Murayama S, Lee EB, Rahimi J, Rodriguez RD, Rozemüller A, Schneider JA, Schultz C, Seeley W, Seilhean D, Smith C, Tagliavini F, Takao M, Thal DR, Toledo JB, Tolnay M, Troncoso JC, Vinters HV, Weis S, Wharton SB, White CL, Wisniewski T, Woulfe JM, Yamada M, Dickson DW (2016) Aging-related tau astrogliopathy (ARTAG): harmonized evaluation strategy. Acta Neuropathol 131:87–102. https://doi.org/10.1007/s00401-015-1509-x

15. Kovacs GG, Lee VM, Trojanowski JQ (2017) Protein astrogliopathies in human neurodegenerative diseases and aging: protein astrogliopathies. Brain Pathol 27:675–690. https://doi.org/10.1111/bpa.12536

16. Kovacs GG, Lukic MJ, Irwin DJ, Arzberger T, Respondek G, Lee EB, Coughlin D, Giese A, Grossman M, Kurz C, McMillan CT, Gelpi E, Compta Y, van Swieten JC, Laat LD, Troakes C, Al-Sarraj S, Robinson JL, Roeber S, Xie SX, Lee VM-Y, Trojanowski JQ, Höglinger GU (2020) Distribution patterns of tau pathology in progressive supranuclear palsy. Acta Neuropathol 140:99–119. https://doi.org/10.1007/s00401-020-02158-2

17. Kundra R, Ciryam P, Morimoto RI, Dobson CM, Vendruscolo M (2017) Protein homeostasis of a metastable subproteome associated with Alzheimer's disease. Proc Natl Acad Sci U S A 114:E5703–E5711. https://doi.org/10.1073/pnas.1618417114

18. Montine TJ, Phelps CH, Beach TG, Bigio EH, Cairns NJ, Dickson DW, Duyckaerts C, Frosch MP, Masliah E, Mirra SS, Nelson PT, Schneider JA, Thal DR, Trojanowski JQ, Vinters HV, Hyman BT, National Institute on Aging, Alzheimer's Association (2012) National Institute on Aging-Alzheimer's Association guidelines for the neuropathologic assessment of Alzheimer's disease: a practical approach. Acta Neuropathol 123:1–11. https://doi.org/10.1007/s00401-011-0910-3

19. Mummery CJ, Börjesson-Hanson A, Blackburn DJ, Vijverberg EGB, De Deyn PP, Ducharme S, Jonsson M, Schneider A, Rinne JO, Ludolph AC, Bodenschatz R, Kordasiewicz H, Swayze EE, Fitzsimmons B, Mignon L, Moore KM, Yun C, Baumann T, Li D, Norris DA, Crean R, Graham DL, Huang E, Ratti E, Bennett CF, Junge C, Lane RM (2023) Tau-targeting antisense oligonucleotide MAPTRx in mild Alzheimer's disease: a phase 1b, randomized, placebo-controlled trial. Nat Med 29:1437–1447. https://doi.org/10.1038/s41591-023-02326-3

20. Nolan A, De Paula Franca Resende E, Petersen C, Neylan K, Spina S, Huang E, Seeley W, Miller Z, Grinberg LT (2019) Astrocytic tau deposition is frequent in typical and atypical Alzheimer Disease presentations. J Neuropathol Exp Neurol 78:1112–1123. https://doi.org/10.1093/jnen/nlz094

21. Perez-Rando M, Dujardin S, Bennett RE, Commins C, Nibhanupudy T, Hyman BT (2020) Synaptic and metabolic gene expression alterations in neurons that are recipients of proteopathic tau seeds. Acta Neuropathol Commun 8:168. https://doi.org/10.1186/s40478-020-01049-7

22. Rexach JE, Cheng Y, Chen L, Polioudakis D, Lin L-C, Mitri V, Elkins A, Yin A, Calini D, Kawaguchi R, Ou J, Huang J, Williams C, Robinson J, Gaus SE, Spina S, Lee EB, Grinberg LT, Vinters H, Trojanowski JQ, Seeley WW, Malhotra D, Geschwind DH (2023) Disease-specific selective vulnerability and neuroimmune pathways in dementia revealed by single cell genomics. bioRxiv 2023.09.29.560245. https://doi.org/10.1101/2023.09.29.560245

23. Roemer SF, Grinberg LT, Crary JF, Seeley WW, McKee AC, Kovacs GG, Beach TG, Duyckaerts C, Ferrer IA, Gelpi E, Lee EB, Revesz T, White CL, Yoshida M, Pereira FL, Whitney K, Ghayal NB, Dickson DW (2022) Rainwater Charitable Foundation criteria for the neuropathologic diagnosis of progressive supranuclear palsy. Acta Neuropathol 144:603–614. https://doi.org/10.1007/s00401-022-02479-4

24. Secci ME, Reed T, Quinlan V, Gilpin NW, Avegno EM (2023) Quantitative analysis of Gene expression in RNAscope-processed brain tissue. Bio Protoc 13:e4580. https://doi.org/10.21769/BioProtoc.4580

25. Simone R, Javad F, Emmett W, Wilkins OG, Almeida FL, Barahona-Torres N, Zareba-Paslawska J, Ehteramyan M, Zuccotti P, Modelska A, Siva K, Virdi GS, Mitchell JS, Harley J, Kay VA, Hondhamuni G, Trabzuni D, Ryten M, Wray S, Preza E, Kia DA, Pittman A, Ferrari R, Manzoni C, Lees A, Hardy JA, Denti MA, Quattrone A, Patani R, Svenningsson P, Warner TT, Plagnol V, Ule J, de Silva R (2021) MIR-NATs repress MAPT translation and aid proteostasis in neurodegeneration. Nature 594:117–123. https://doi.org/10.1038/s41586-021-03556-6

26. Takanashi M, Mori H, Arima K, Mizuno Y, Hattori N (2002) Expression patterns of tau mRNA isoforms correlate with susceptible lesions in progressive supranuclear palsy and corticobasal degeneration. Brain Res Mol Brain Res 104:210–219. https://doi.org/10.1016/s0169-328x(02)00382-0

27. Wang F, Flanagan J, Su N, Wang L-C, Bui S, Nielson A, Wu X, Vo H-T, Ma X-J, Luo Y (2012) RNAscope J Mol Diagn 14:22–29. https://doi.org/10.1016/j.jmoldx.2011.08.002

28. Whitney K, Song W-M, Sharma A, Dangoor DK, Farrell K, Krassner MM, Ressler HW, Christie TD, Walker RH, Nirenberg MJ, Zhang B, Frucht SJ, Riboldi GM, Crary JF, Pereira AC (2023) Single-cell transcriptomic and neuropathologic analysis reveals dysregulation of the integrated stress response in progressive supranuclear palsy. bioRxiv 2023.11.17.567587. https://doi.org/10.1101/2023.11.17.567587

29. Zhang Y, Sloan SA, Clarke LE, Caneda C, Plaza CA, Blumenthal PD, Vogel H, Steinberg GK, Edwards MSB, Li G, Duncan JA, Cheshier SH, Shuer LM, Chang EF, Grant GA, Gephart MGH, Barres BA (2016) Purification and characterization of progenitor and mature human astrocytes reveals transcriptional and functional differences with Mouse. Neuron 89:37–53. https://doi.org/10.1016/j.neuron.2015.11.013

Publisher's Note